frontiers | Frontiers in Marine Science

TYPE Original Research
PUBLISHED 09 February 2023
DOI 10.3389/fmars.2023.1141187



OPEN ACCESS

EDITED BY
Yifei Zhao,
Nanjing Normal University, China

REVIEWED BY
Mao Longjiang,
Nanjing University of Information Science and Technology, China
Mingming Ma,
Fujian Normal University, China

*CORRESPONDENCE
Longsheng Wang
52wls@163.com

SPECIALTY SECTION
This article was submitted to Coastal Ocean Processes, a section of the journal Frontiers in Marine Science

RECEIVED 10 January 2023
ACCEPTED 27 January 2023
PUBLISHED 09 February 2023

CITATION
Meng L, Wang L, Zhao J, Zhan C, Liu X, Cui B, Zeng L and Wang Q (2023) End-member characteristics of sediment grain size in modern Yellow River delta sediments and its environmental significance.
*Front. Mar. Sci.* 10:1141187.
doi: 10.3389/fmars.2023.1141187



# End-member characteristics of sediment grain size in modern Yellow River delta sediments and its environmental significance

Liwei Meng[1], Longsheng Wang[1,2,3,4]*, Jiawen Zhao[1], Chao Zhan[1], Xianbin Liu[1], Buli Cui[1], Lin Zeng[1] and Qing Wang[1]

[1]Institute of Coastal Research, Ludong University, Yantai, China, [2]Key Laboratory of Coastal Environmental Processes and Ecological Remediation, Yantai Institute of Coastal Zone Research, Chinese Academy of Sciences, Yantai, China, [3]State Key Laboratory of Loess and Quaternary Geology, Institute of Earth Environment, Chinese Academy of Sciences, Xi'an, China, [4]State Key Laboratory of Lake Science and Environment, Nanjing Institute of Geography and Limnology, Chinese Academy of Sciences, Nanjing, China

**Introduction:** The sediments of the Yellow River delta record the environmental changes in the Yellow River basin on a long time scale and are sensitive to the river diversion and sedimentary environment evolution.

**Methods:** In this study, cores YDC and YDG in the delta near the estuary of the Yellow River since 1976 were taken as the research object, and the parameterized end-member analysis model was used to analyze the grain-size data of the cores.

**Results:** The results show that: The main sediments were silty and sand (58% and 77.9%). The grain-size parameters showed opposite changes with wide grain-size ranges and mixed sizes obviously. End member 1 (EM1) and end member 2 (EM2) were composed of clay and fine silt with fine particle sizes of 0.04 mm and 9.8 mm, respectively, and were deposited under weak hydrodynamic conditions during long-distance transport along the Yellow River. End member 3 (EM3) and end member 4 (EM4) were coarse silt with mode particle sizes of 40.14 mm and 66.89 mm, respectively. These were deposited by waves and tidal currents under strong dynamic conditions.

**Discussion:** According to the channel changes and the sedimentary facies data of the modern Yellow River delta, before the Yellow River was diverted in 1996, the cores YDC and YDG were both in the estuary-front bar sedimentary environment. In 1996, the Yellow River was diverted to the Qing 8 course. Subsequently, the core YDC changed to the delta-plain sedimentary facies, and the core YDG changed to the delta-front facies. The sediment sources of the two cores changed from the Yellow River sediments to coastal sediment erosion and resuspension. The sedimentary environment changed from siltation to erosion. The results of this study are of great practical significance for estuary management and coastal engineering construction in the modern Yellow River delta and can provide a scientific basis for ecological protection and high-quality development of the Yellow River basin.

KEYWORDS

**grain-size characteristics, end-member analysis, river channel change, sedimentary environment, Yellow River delta**

# 1 Introduction

The delta is a sensitive geomorphic unit at the intersection of the lithosphere, hydrosphere, biosphere, and atmosphere (Hu et al., 2021), which is influenced by the coupling effects of river water, sediment, and ocean dynamics (Chen T, et al., 2021; Wang et al., 2019). The delta also supports more than 500 million people around the world by providing fertile soil and rich natural resources (Milliman and Meade, 1983; Jia et al., 2011; Dethier et al., 2022). The modern Yellow River delta formed due to rapid sedimentation and artificial diversion into the Bohai Sea in 1885 (Han et al., 2011; Wu et al., 2017). The important social and economic value of the modern Yellow River delta as well as its unique ecological environment, development pattern, and influence mechanism have attracted significant attention from scholars. Recently, owing to the influence of river diversion and ocean dynamics, significant changes in the sediment flow into the Yellow River mouth have occurred (Liu et al., 2012; Li et al., 2015). The sediment composition of the Yellow River mouth records the influence of natural and human activities, such as river channel changes and ocean dynamics (Hou et al., 2021). Therefore, study of the Yellow River mouth sediments provided a new understanding of the geomorphic evolution and dynamic changes of the modern Yellow River delta region (Wu et al., 2020). However, the Yellow River mouth location change and its complex sedimentary environment make it difficult to date the Yellow River mouth location, resulting in a lack of continuous sedimentary records for the Yellow River mouth sediments (Wang et al., 2010).

Grain-size analysis has been widely used in sedimentology and paleoenvironmental analysis. By studying the sediment grain sizes in the modern Yellow River delta, their material sources and transport dynamics can be analyzed to characterize the sedimentary environment changes (Xu, 2000; Wang et al., 2018; Varga et al., 2019). However, due to the diversity of sediment sources, the variability of transport forces, and the complexity of the sedimentary environment, the interpretation of grain size has complexity and uncertainty with respect to its environmental significance Chen H, et al., 2021 (Jiang et al., 2018; Van Hateren et al., 2018; Wen et al., 2019). The grain size end-member analysis can decompose sediment grain size into several end members related to specific deposition process with specific grain size characteristics distribution. In addition to reducing human errors, the characteristic end members can be placed on the time series to judge the changes of environmental factors. By placing the separated grain size end members on the spatial plane, we can effectively identify the end-member information that can reveal the source of sediment material and the combination characteristics of sedimentary dynamic components. Zang et al., 2015 Therefore, it has been widely used to study the evolution of sedimentary environment, provenance identification and human activity indication in estuarine deltas (Chen et al., 2020; Liu M, et al., 2021; Liu R, et al., 2021; Wang et al., 2017; Wen et al., 2019). Zhang et al. (2006) used the end-member analysis (EMA) model to analyze the sediment grain-size data in the sea areas adjacent to the Yangtze River mouth, and understood the transport mechanism and settlement behavior of sediments in the Yangtze River mouth region. Paladino et al. (2022) used the end-member analysis model to analyze the sediments of the Paranaguá Estuarine Complex and more accurately understand the effects of hydrodynamic processes on the sediment distribution and deposition process. Wang et al. (2021) adopted the grain-size end-member analysis method and combined it with the grain-size parameters of the sediments, the water depth of the study area, and the hydrodynamic factors to analyze and judge the sedimentary dynamics of surface-sediment samples in Quanzhou Bay, Fujian Province; their work quantified the complex sedimentary dynamic characteristics of the surface sediments in the study area. Considering that there are relatively few studies on grain-size end members of sediments in the modern Yellow River delta, this study takes cores YDC and YDG at the mouth of the modern Yellow River delta as the research object, analyzes the characteristics of grain-size end members of sediments, and discusses the environmental significance of grain-size end-member characteristics. The research results provide guidance for the planning, management, and engineering construction of the modern Yellow River delta, and provide a scientific basis for the protection and sustainable development of the modern Yellow River delta.

# 2 Study area

The modern Yellow River delta is bordered by the Bohai Bay in the north and the Laizhou Bay in the east. With Ninghai in Kenli County as its axis point (Figure 1). The modern Yellow River delta has a semi-humid continental monsoon climate in the warm temperate zone. It is hot and rainy in summer and cold and dry in winter. The prevailing wind is north or northeast and the average annual precipitation is 530–630 mm. According to the statistical data from Lijin Hydrology Station in the Yellow River mouth, the annual average runoff is $3.22\times10^{10}$ $m^3$, and the annual average sediment transport is $8.39\times10^{8}$ $m^3$ (Zhang J, et al., 2020). Owing to the influence of weak dynamics such as tides and storm surges in the mouth, most sediments are deposited in the delta or near the coastline. However, due to the influence of human activities such as water resource development, reservoir construction, or water and sand diversion, the sediment carried by the Yellow River into the sea has decreased year by year (Dethier et al., 2022).

# 3 Materials and methods

## 3.1 Sample collection and testing

In 2018, cores YDC (119°11′17.03″E, 37°44′37.88″N) and YDG (119°11′20.01″E, 37°44′26.35″N) were collected near the southern branch of the Qing 8 course of the modern Yellow River delta (Figure 1). Combined with the results of Shi (2021), we determined the sedimentary facies of the two cores are delta-plain and delta-front facies using the sedimentary structure, color and other characteristics of the core sediments. There was a significant erosion interface at 28 cm, the underlying layer of the two cores are yellowish-gray silty clay, which belonged to the Yellow River sediment input (Wu et al., 2020), and the overlying layers are bluish-gray silty sand, combined with previous research results, it was identified as sediment under the

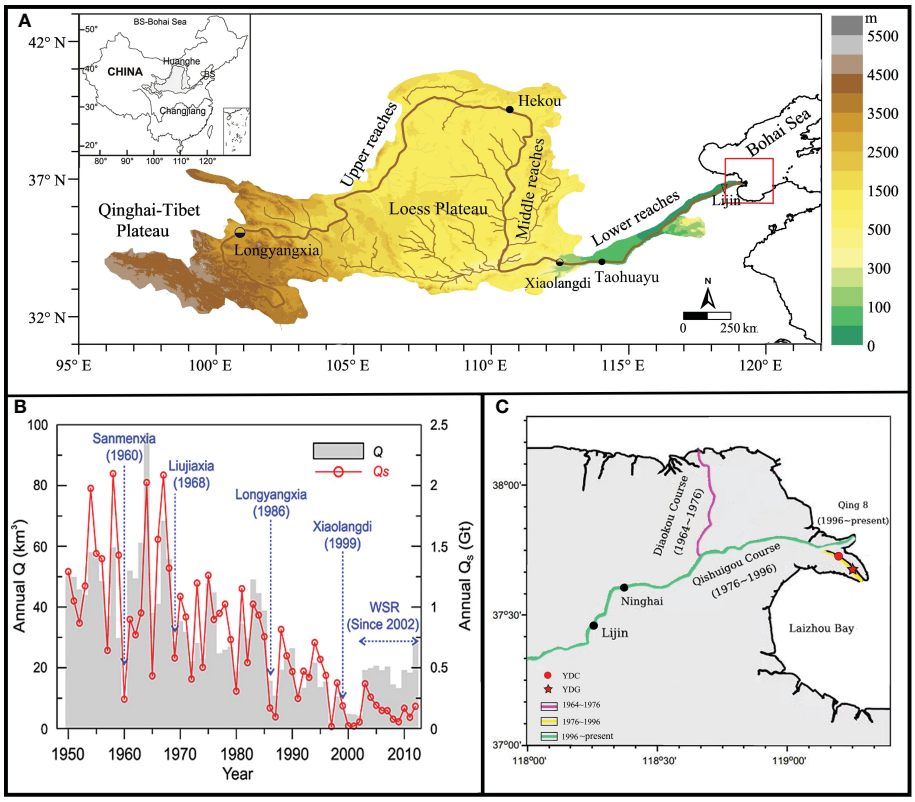


FIGURE 1
**(A)** Map of the Yellow River basin (Liu et al., 2022). **(B)** Annual water and sediment discharges from the Yellow River to the sea recorded at Lijin Station, 1950–2012. WSR is the Water–Sediment Regulation Scheme since 2002 (Hu et al., 2015). **(C)** Map of river channel changes and core locations in the Yellow River delta (Wu et al., 2020).

action of ocean dynamics (Hou et al., 2021). We determined that the sediment above 28 cm was the sediment input from the Yellow River which was diverted to clear the ditch before 1996. The elevation of two cores were 1.5 m, and the depths of the cores were 100 cm. In the laboratory, samples were divided at intervals of 2 cm. The grain-size samples were tested in the Coastal Institute of Ludong University using the Mastersizer 3000 laser grain-size analyzer. The test range was 0.01–2000 μm, and the relative error was less than 2%. Hydrogen peroxide ($H_2O_2$) and hydrochloric acid (HCl) were added to remove organic matter and carbonate ($CaCO_3$), respectively. Finally, sodium hexametaphosphate ($(NaPO_3)_6$) solution was added as the dispersant. After 7 min of ultrasonic vibration, measurements were carried out on the computer.

## 3.2 Data analysis

In this paper, the Udden–Wentworth grain-size scale was used to divide the sediments into <4 μm (clay), 4–63 μm (silt), and >63 μm (sand); the silt was further divided into 4–8 μm (very fine silt), 8–16 μm (fine silt), 16–32 μm (medium silt), and 32–63 μm (coarse silt). In this study, the grain-size end-member analysis was carried out by loading the AnalySize program developed by Paterson and Heslop (2015) in Matlab, and the Gen.Weibull was selected for grain-size end member (EM) decomposition (Paterson and Heslop, 2015). The criteria for determining the number of end members are the degree of fit ($R^2$) (linear solutions indicate correlation between the original granularity data set and the metadata at the fitting end) and angle (θ) (angular deviation, end metadata and grain-size curve distribution deviation). Under the premise of a good fitting effect and no over-fitting, the number of selected end members should be as few as possible (Zhang X, et al., 2020).

# 4 Results and analysis

## 4.1 Grain-size characteristics

Grain size is a basic characteristic of sediment, and its composition is related not only to that of the parent material but also to the sedimentary environment, which can directly reflect the content and distribution characteristics of mechanical components (Pan et al., 2015; Zhong et al., 2020). It can be seen from the grain-size composition of cores YDC and YDG that the sediments in the modern Yellow River delta are mainly silty sand (4–63 μm) (Figure 2). The content of silt (4-63 μm) in core YDC ranges from 20.28% to 82.83%, with an average of 58.47%, and the content of clay (<4 μm) ranges from 6.57% to 79.26%, with an average of 36.9%. Sand (>63 μm) ranges from 0.01% to 15.98%, with an average content of 4.62%. The content of silt (4-63 μm) in core YDG ranges from 17.14% to 82.35%, with an average of 67.6%. The content of clay (<4 μm) ranges from 5.51% to 92.18%, and the average content was 21.72%.

10.3389/fmars.2023.1141187

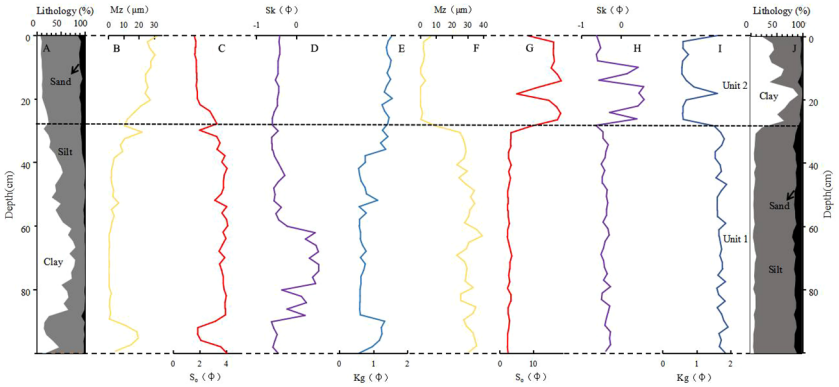


FIGURE 2
Characteristics of grain-size parameters with depth for cores YDC **(A–E)** and YDG **(F–J)**.

Sand (>63 μm) ranges from 0.7% to 17.3%, with an average content of 10.68%. For the two cores, the compositions of clay grains, silty sand, and sand at different depths show opposite trends. The maximum values of clay (<4 μm) in cores YDC and YDG appeared in Unit 1 (28–100 cm) and Unit 2 (0–28 cm), respectively. The maximum value of silt (4–63 μm) appear in Unit 2 (0–28 cm) and Unit 1 (28–100 cm), respectively, while the maximum values of sand (>63 μm) appear in Unit 2 (0–28 cm) and Unit 1 (28–100 cm), respectively.

The sediment grain-size parameters indicate sedimentary environmental condition changes (Liu et al., 2012; Li et al., 2019). The grain-size parameters of cores YDC and YDG are shown in Table 1 and Figure 2. The maximum and minimum mean grain sizes (Mz) of core YDC are 32.17 μm and 0.28 μm, respectively, located in Unit 2 (0–28 cm) and Unit 1 (28–100 cm). The maximum and minimum mean grain sizes (Mz) of core YDG are 35.64 μm and 0.08 μm, respectively, located in Unit 1 (28–100 cm) and Unit 2 (0–28 cm), suggesting the variations of sediment dynamics and provenance at different depths. In the cores YDC and YDG, the sorting coefficient (σ) values are between 1.57–4.1 and 2.21–18.89, respectively, with poor sorting performance. The skewness (Sk) values in cores YDC and YDG were between −0.62–0.56 and −0.63–0.58, respectively, with the mean values of −0.27 and −0.29 The kurtosis (Kg) values in cores YDC and YDG are between 0.57–1.56 and 0.58–1.88, respectively, indicating narrow kurtosis.

The grain-size distribution frequency curve and cumulative frequency curve can reflect the sedimentary characteristics of the whole sample and directly show the distribution characteristics (Liu et al., 2021). The grain-size distribution frequency curves of core YDC (Figures 3A, B) show three peaks, with grain size mainly concentrated in the silt range. The first and second peak values are 0.02–0.06 μm and 0.4–0.8 μm, respectively, indicating clay components. The third peak values are 20–52 μm, indicating silt composition. In addition to the trimodal state of sample YDG11, the grain-size compositions of core YDG present a bimodal state (Figure 3C), with relatively dispersed grain-size compositions and poor sorting. The first peak of core YDG is 0.5–0.7 μm, indicating clay composition, and the second peak is 29–37 μm, indicating silt composition. The grain-size accumulation frequency curves show that the slope of the core YDC curve (Figure 3B) is basically the same as that of the core YDG (Figure 3D) but deviates toward the coarse component suggesting the change of transport medium and dynamic conditions.

TABLE 1 Characteristics of the grain-size parameters of each stratum in the cores YDC and YDG, and comparison of the mean value of EMA results within different units.

| | YDC | | YDG | |
|---|---|---|---|---|
| | Unit2(0-28cm) | Unit1 (28-100cm) | Unit 2(0-28cm) | Unit1 (28-100cm) |
| Mz (μm) | 23.85 | 4.97 | 2.25 | 30.04 |
| Md (μm) | 28.51 | 8.11 | 5.87 | 34.53 |
| So(φ) | 2.01 | 3.5 | 14.45 | 2.78 |
| Sk(φ) | -0.48 | -0.2 | -0.09 | -0.39 |
| Kg(φ) | 1.43 | 0.84 | 0.84 | 1.71 |
| EM1 (%) | 1.34 | 33.75 | 44.48 | 0.55 |
| EM2 (%) | 27.40 | 40.01 | 34.33 | 20.07 |
| EM3 (%) | 30.31 | 19.33 | 19.03 | 15.17 |
| EM4 (%) | 40.95 | 6.90 | 2.16 | 63.54 |

10.3389/fmars.2023.1141187

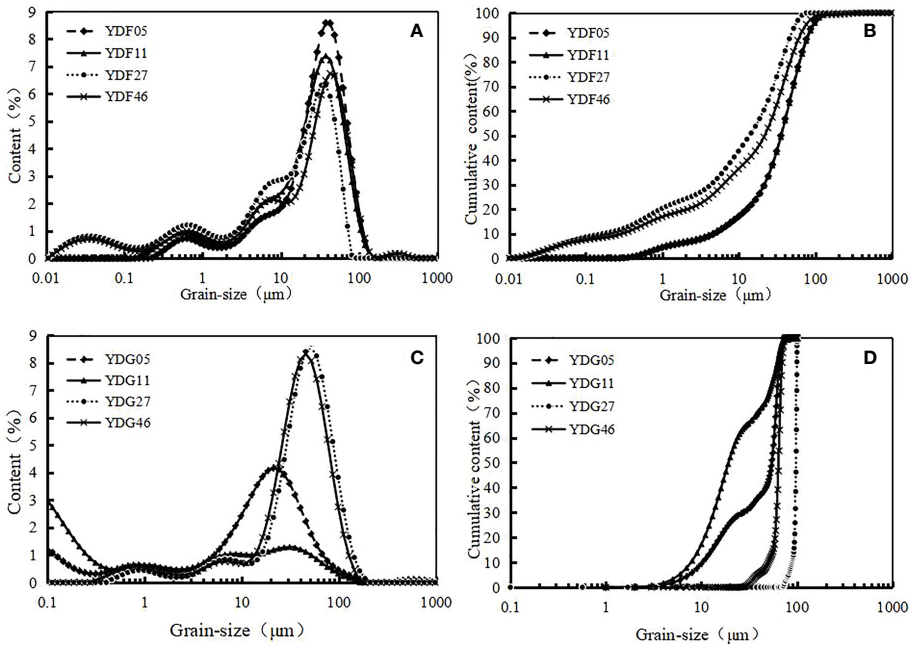


FIGURE 3
Grain-size distribution **(A, C)** and accumulative frequency curves **(B, D)** of cores YDC **(A, B)** and YDG **(C, D)**.

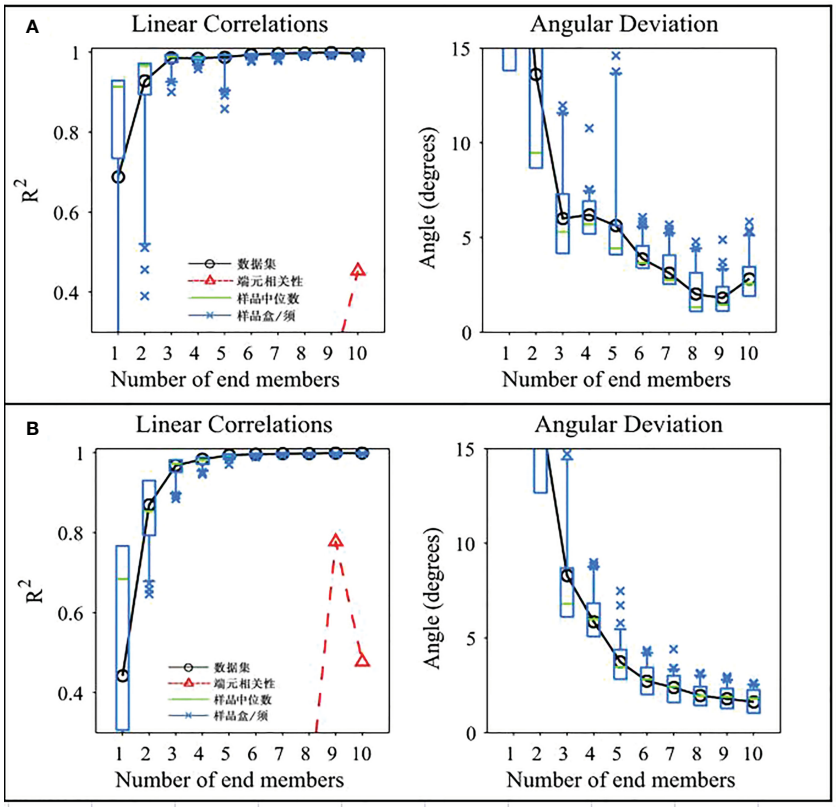


FIGURE 4
Results of parametric end-member analysis of cores YDC **(A)** and YDG **(B)**. **(A)** The squared linear correlation ($R^2$). **(B)** The angular distance in degrees (Theta).

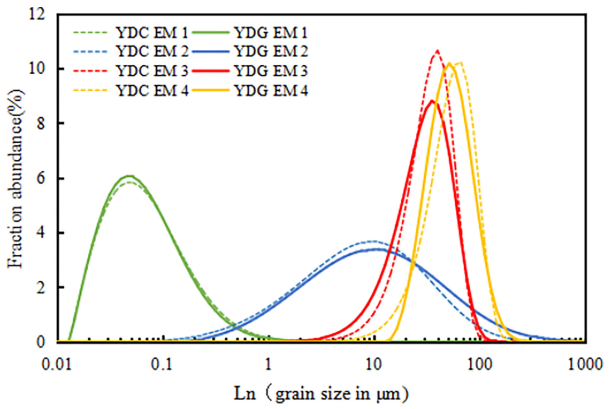


FIGURE 5
Parametric end-member frequency distribution curves.

## 4.2 Grain-size end-member analysis

The grain-size data of the YDC and YDG core samples were parameterized by the AnalySize program, and the index results of different end members were compared (Chen et al., 2021). It was found that the fitting effect of the grain-size curve and the end member was better with an increased number of end members (Wen et al., 2019). The parameterized results with four end members of core YDC are $R^2$ = 0.98 with the angle deviation of θ = 5.9 (Figure 4). The parameterized results with four end members of core YDG are $R^2$ = 0.99 with the angle deviation of θ = 6.2, indicating that the fitting requirements can be met for these conditions. When the number of end members is 5 or 6 (Figure 4), the $R^2$ of core YDC is 0.99 or 0.99, and the angle deviation θ is 3.7 or 2.7, respectively; the $R^2$ of core YDG is 0.99 or 0.99, and the angle deviation θ is 5.6 or 3.9, respectively. The improvements are not obvious when the values are compared with those of four end members. According to the principle of selecting the smallest number of end members to meet the optimal fitting, this study selected four end members for analysis.

According to the end-member frequency distribution curve and the correlation analysis of each grain-size end member with grain-size components and parameters (Figure 5; Table 1) (Van Hateren et al., 2018; Wen et al., 2019; Zhang et al., 2020), the grain sizes of the four end-member modes in core YDC are as follows: end member 1 (EM1) = 0.05 μm, clay; end member 2 (EM2) = 9.9 μm, fine silt; end member 3 (EM3) = 40.14 μm, coarse silt; and end member4 (EM4) = 66.89 μm, sand. The four end-member modes of core YDG are EM1 = 0.04 μm, clay, EM2 = 8.68 μm, fine silt, EM3 = 31.1 μm, coarse silt; and EM4 = 45.61 μm, sand. Both the end-member grain-size distribution frequency curves of cores YDC and YDG are unimodal. EM1 and EM2 have wide peak areas, large distribution ranges, and relatively poor sorting; EM3 and EM4 have high peak values, narrow peak areas, and good sorting. These results indicate that the source areas of the EM1 and EM2 sediments are far away and the sediment is transported over a long distance, while the source areas of EM3 and EM4 sediments are close and the transport distance is short (Wu et al., 2017).

According to the variation of each end member with depth (Figure 6), the variation range of EM1 in the whole core YDC is 0.004%–67.81%, with an average value of 23.34%, and the variation range of EM2 is 13.3%–56.17%, with an average value of 36.46%. EM3 varies from 2.42% to 63.04% with an average value of 23.09%, while EM4 varies from 0% to 50.12% with an average value of 17.11% (Table 1). In core YDG, EM1 varies from 0% to 84.14% with an average value of 13.09%, EM2 varies from 10.2% to 41.76% with an average value of 24.3%, and EM3 varies from 0% to 53.83% with an average value of 16.25%. EM4 varies from 0% to 78.2%, with an average value of 46.35%.

# 5 Discussion

## 5.1 Environmental significance of grain-size endmembers

To explore the environmental significance of each end member, it is necessary to further clarify the relationship between the end member and the traditional granularity index. In this study, SPSS software was used to analyze the correlation between each grain-size end member and the grain-size components and parameters, as shown in Table 2.

The mean grain size (Mz) of core YDC is negatively correlated with EM1 and EM2, and positively correlated with EM3 and EM4. The average grain size of core YDG is negatively correlated with EM1, EM2, and EM3, and positively correlated with EM4, indicating a significant difference in the coarseness of end-member grain size. The grain size of core YDG is coarser, which reflects the strength of sedimentary dynamics between different end members at different the core locations. The sorting coefficient (σ) of core YDC is positively correlated with EM1 and EM2, and negatively correlated with EM3 and EM4. The sorting coefficient (σ) of core YDG is positively correlated with EM1, EM2 and EM3 and negatively correlated with EM4, further demonstrating the poor sort of EM1 and EM2 and the relatively dispersed particle size distribution associated with the presence of multiple fine grain-size peaks. The kurtosis (Kg) of core YDC is negatively correlated with EM1 and EM2, and positively correlated with EM3 and EM4. The kurtosis (Kg) of core YDG is significantly negatively correlated with EM1 and EM2, negatively correlated with EM3, and positively correlated with EM4. These correlations correspond to the main peak widths of the frequency distribution curves of EM1 and EM2 and the main peak tips of EM3 and EM4, reflecting that the sedimentary environments of EM3 and EM4 are relatively stable. The correlation analysis of grain-size end members and grain-size components showed that there were significant positive correlations between EM1 and clay in both cores YDC and YDG ($R^2$ = 0.99), positive correlations between EM2 and clay, and negative correlations between EM1 and EM2 and silt and sand compositions. EM3 was positively correlated with silt and negatively correlated with clay. EM4 was positively correlated with sand ($R^2$ = 0.97 and $R^2$ = 0.95) and negatively correlated with clay. These results indicate that the grain-size distribution ranges of each end member are closely related to the grain-size components, that is, EM1 and EM2 are mainly clay, EM3 is mainly silty sand, and EM4 is mainly sand. The results of end-member correlation analysis showed that EM1 was positively correlated with EM2, and negatively correlated with EM3 and EM4, indicating that the material sources and influencing factors of EM1 and EM2 were consistent, and that

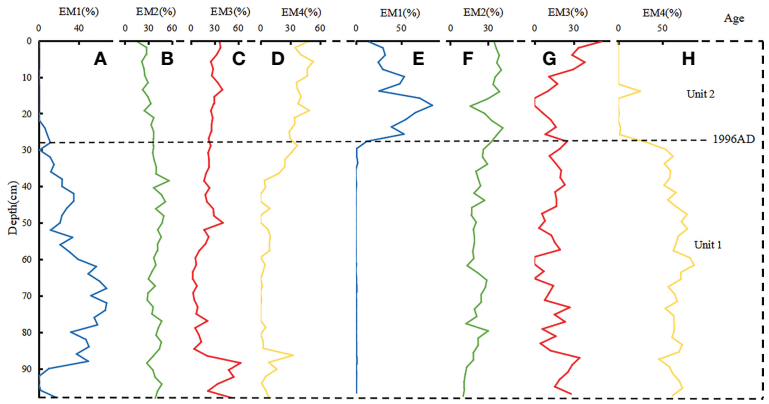


FIGURE 6
Depth distributions of the relative contents of the four EMs of the sediments from cores YDC **(A–D)** and YDG **(E–H)**.

those of EM3 and EM4 were consistent. Previous studies have shown that the sediment composition of the Yellow River mouth is mainly composed of clay and fine silt, while the content of coarse silt and sand is relatively low (Li, 1989; Li et al., 2013; Yuan et al., 2016). Based on results, we conclude that EM1 and EM2 were deposited under weak hydrodynamic conditions during the long-distance transport of the Yellow River, while EM3 and EM4 are near-source sediments under the action of strong hydrodynamic waves and tidal currents (Wu et al., 2021).

## 5.2 Analysis of transport dynamics and sedimentary environment evolution

According to the grain-size parameters, grain-size end-member analysis, and sedimentary characteristics changes of core YDC and YDG in the modern Yellow River delta, the two cores are divided into two parts: Unit 1 (28–100 cm) and Unit 2 (0–28 cm). There was an obvious change in the two cores at 28 cm, and the grain sizes of the sediments and the grain-size end members showed that the difference above and below 28 cm was opposite in both cores, the underlying layer was yellowish-gray silty clay, which belonged to the Yellow River sediment input, and the overlying layer was bluish-gray silty sand, combined with previous research results, it was identified as sediment under the action of ocean dynamics (Hou et al., 2021). By combining the vertical grain-size changes of the two cores to analyze their formation ages, it is determined that the layer at 28–100 cm was formed before the diversion of the Yellow River in 1996, and the layer at 0–28 cm was formed between 1996 and 2018. Unit 1 (28–100 cm) of core YDC is mainly composed of clay and silty sand, classified as silty clay; while the core YDG (28–100 cm) is mainly composed of silty sand, which is a typical Yellow River sediment. The calculated deposition rate is 1.27 cm/yr. Through $^{210}$Pb dating analysis of borehole core sediments in adjacent areas, Wu et al. (2020) found that $^{210}$Pbex dropped steadily from 0 cm to 38 cm in the core, showing the best fitting linear regression (correlation coefficient $R^2 = 0.75$; Wu et al., 2020). Therefore, the estimated average deposition rate was 1.85 cm/yr, which was consistent with the results of this study. The reliability of using grain-size changes as a dating method is proved by the fact that silt and sand are the main components, and the sand content is significantly increased by 80% compared with that of Unit 1 (28–100 cm). In core YDG, clay is the main component, and silt and sand are significantly reduced. It is inferred that since the diversion of the Yellow River to the Qing 8 course in 1996, the source of sediment in the Yellow River delta has changed, and the sediment content of clay and fine silt has decreased rapidly (Hu et al., 2020). Owing to the different locations of cores YDC and YDG, the sedimentary environment and sedimentary facies are significantly different, resulting in the obvious opposite grain-size changes in the two cores.

The complex sediment deposition process of the modern Yellow River delta is influenced by the hydrodynamics and the comprehensive actions of various transport forces (Chen et al., 2021; Xue et al., 2009; Shi, 2021). The sediment quantity, transport mode, and grain size of the river mouth all have obvious influences on the sedimentary facies and development processes of the delta area (Shi, 2021). The sedimentary facies of the modern Yellow River delta are mainly divided based on grain-size composition, color characteristics, and development history. The basic sedimentary facies are the delta-plain, delta-front, and predelta facies (Wu et al., 2020). Through the analyses of the grain-size parameters, grain-size end-member metadata, and sedimentary characteristics of cores YDC and YDG, the contents of clay, silt, and sand in core YDC are determined as 37.1%, 58.2%, and 4.7%, respectively; the contents of clay, silt, and sand in core YDG are determined as 21.7%, 67.6%, and 10.7%, respectively. Compared with core YDC, the clay content of core YDG is reduced by 15.4%, the silt content is increased by 9.4%, and the sand content is increased by 6%, which is basically consistent with the analysis of Shi (2021) that the sediment grain sizes of the delta-front facies at the Yellow River mouth had reduced clay content and increased sand content, while the silt content remained the same. Therefore, we inferred that cores YDC and YDG were located in delta-plain facies before 1996 (Figure 7). After the Yellow River divered in 1996, the core YDC and core YDG were located in delta-plain facies and delta-front facies, respectively (Figure 7). Since the diversion of the Yellow River to the Qing 8 course in 1996, the sedimentary environment of the modern Yellow River delta has been changing continuously due to the influence of channel migration and other factors. The grain-size characteristics of cores YDC and YDG have well recorded and responded to these changes.

Unit 1 (28–100 cm) was formed before the Yellow River was diverted to the Qing 8 course in 1996. The sediments of the two cores

10.3389/fmars.2023.1141187

TABLE 2 Correlation analysis of each grain-size end member with grain-size components and parameters of cores YDC and YDG.

| | | Clay | Silt | Sand | EM 1 | EM 2 | EM 3 | EM 4 | Mz | So | Sk | Kg |
|---|---|---|---|---|---|---|---|---|---|---|---|---|
| YDC | Clay | 1 | | | | | | | | | | |
| | Silt | -0.99** | 1 | | | | | | | | | |
| | Sand | -0.8** | 0.71** | 1 | | | | | | | | |
| | EM 1 | 0.99** | -0.99** | -0.74** | 1 | | | | | | | |
| | EM 2 | 0.39** | -0.32** | -0.61** | 0.29* | 1 | | | | | | |
| | EM 3 | -0.8** | 0.9** | 0.33* | -0.83** | -0.21 | 1 | | | | | |
| | EM 4 | -0.82** | 0.74** | 0.97** | -0.75** | -0.68** | 0.36** | 1 | | | | |
| | Mz | -0.89** | 0.85** | 0.85** | -0.84** | -0.72** | 0.64** | 0.91** | 1 | | | |
| | So | 0.83** | -0.81** | -0.72** | 0.78** | 0.68** | -0.69** | -0.78** | -0.96** | 1 | | |
| | Sk | 0.83** | -0.85** | -0.52** | 0.87** | -0.06 | -0.72** | -0.5** | -0.5** | 0.4** | 1 | |
| | Kg | -0.88** | 0.84** | 0.83** | -0.84** | -0.61** | 0.63** | 0.86** | 0.89** | -0.71** | -0.57** | 1 |
| YDG | Clay | 1 | | | | | | | | | | |
| | Silt | -0.92** | 1 | | | | | | | | | |
| | Sand | -0.89** | 0.83** | 1 | | | | | | | | |
| | EM 1 | 0.99** | -0.99** | -0.87** | 1 | | | | | | | |
| | EM 2 | 0.57** | -0.53** | -0.63** | 0.51** | 1 | | | | | | |
| | EM 3 | -0.11 | 0.21 | -0.27 | -0.15 | 0.16 | 1 | | | | | |
| | EM 4 | -0.89** | 0.84** | 0.95** | -0.86** | -0.75** | 0.31** | 1 | | | | |
| | Mz | -0.91** | 0.86** | 0.94** | -0.88** | -0.8** | -0.19** | 0.98** | 1 | | | |
| | So | 0.8** | -0.76** | -0.83** | 0.77** | 0.83** | 0.17** | -0.9** | -0.92** | 1 | | |
| | Sk | 0.75** | -0.8** | -0.5** | 0.78** | -0.06 | -0.44** | -0.45** | -0.45** | 0.36** | 1 | |
| | Kg | -0.8** | 0.76** | 0.78** | -0.77** | -0.77** | -0.07 | 0.84** | 0.86** | -0.96** | -0.44** | 1 |

** At level 0.01 (two-tailed), the correlation was significant.
* At level 0.05 (two-tailed), the correlation was significant.

were mainly clay and silty sand, which was the sedimentary environment of the delta-front mouth bar. The sediment carried by the Yellow River was a stable source of sediment supply in this region. Approximately 90% of the Yellow River sediment comes from the Loess Plateau, and the content of silt and clay in the sediment is high (Wu et al., 2021). In Unit 1, the contents of clay and silt in the core YDC are 46.8% and 50.7%, respectively. The contents of clay and silt in core YDG are 8.4% and 77.8%, respectively. Core YDC in the delta-plain sedimentary facies is mainly dominated by fluvial sediments, including riverbed and floodplain, etc. The sedimentary environment and hydrodynamic conditions are greatly changed, and the contents of the three grain-size groups are consistent with the sediments from the mouth (Wang et al., 2017). The average contents of EM1 and EM2 representing the Yellow River sediment components in Unit 1 are

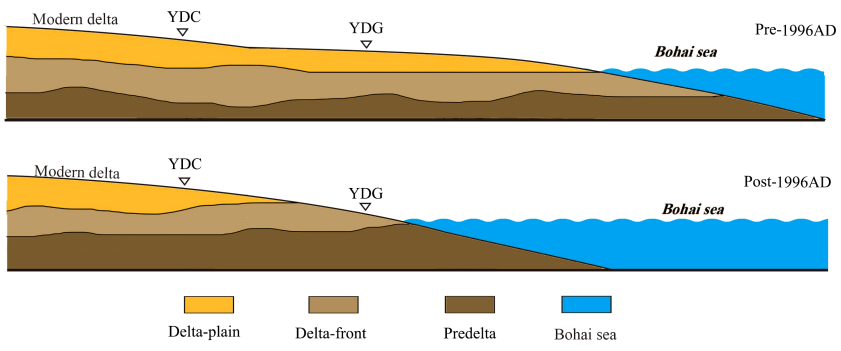


FIGURE 7
Sedimentary facies variation in the Yellow River Delta around 1996 (Zeng et al., 2022).

33.75% and 40.01%, respectively. Core YDG in the delta -front facies is in the mouth area, which has the fastest deposition in the delta system. It is subject to the alternating action of sedimentation and erosion by the river and ocean, and the sedimentary environment is complex (Xue et al., 2009). The sediments are derived from the erosion and resuspension of the Yellow River sediments and the coastal sediments, and they are significantly affected by the strong tidal and wave hydrodynamics (Wang et al., 2017), making the sediment grain size be coarser. In Unit 1 (28–100 cm), the silty sand content accounted for 77.8%, an increase of 20.1% compared with that of the core YDC, representing the average EM3 and EM4 contents of coarse grain components were 15.2% and 66.5%, and the average EM1 and EM2 contents of fine grain components were 0.6% and 20%.

Unit 2 (0–28 cm) was formed from 1996 to 2018. In 1996, the Yellow River was diverted to the Qing 8 course, and the sediment source of the two cores changed. The Yellow River sediments rapidly decreased, the clay and silt contents also decreased, and the sedimentary environment changed from siltation to erosion (Zhang et al., 2022), and these changes are well documented in the core YDC, which is located in the plain sedimentary phase. In Unit 2, the clay content of core YDC decreased rapidly by 35.4%, and the silty sand content increased by 28.6%. The sand content increased by 80%. Simultaneously, the EM3 and EM4 contents representing the coarse-grained components increased rapidly, reaching 30% and 40.2%, respectively. The EM1 and EM2 components representing fine-grained components decreased rapidly, with average contents of 1.3% and 27.3%, respectively. However, owing to the different sedimentary facies locations, the grain-size changes of core YDG are obviously opposite to that of core YDC. In core YDG, the clay content increases rapidly with an average content of 55.9% and an increase of 85%, while the silty sand and sand decrease further with average contents of 41.2% and 2.8%, respectively, representing the rapid increase of EM1 and EM2 fine-grained components, the mean coarse-grained contents of EM3 and EM4 were 44.5% and 34.3%, respectively. The mean coarse-grained contents of EM3 and EM4 were 19% and 2.2%, respectively. The core YDG was in the delta-front facies, and combined with previous studies, Qiao et al. (2010) found that highly overhanging sand areas are present in the current mouth and at the delta-front of the old Qingshuigou mouth, and that the seabed surface sediments were mainly composed of fine silt and clay silt. Li et al. (1998) found that the delta-front was significantly affected by marine action, and most of the delta-front was covered by the slope of the delta-front, which was dominated by tidal currents for suspended sediment dispersal and deposition, resulting in a fast deposition rate, mainly consisting of fast settling fine sandy clay, and its sediment was mainly composed of powdery clay and clayey chalk with high water content (McCave and Swift, 1976), which better confirmed the difference in sediment grain-size between cores YDG and YDC.

## 6 Conclusion

The grain-size components and end members of cores YDC and YDG in the modern Yellow River delta clearly record the channel changes and sedimentary environment changes in the Yellow River basin.

Analysis of traditional grain-size parameters has shown that the sediments of cores YDC and YDG are mainly silty sand. The average grain-size composition of core YDC is silty sand (58.14%) > clay (37.15%) > sand (4.69%), and that of core YDG is silty sand (67.59%) > clay (21.71%) > sand (10.68%). The sand content of core YDC is mainly concentrated in Unit 2 (0–28 cm) and that of core YDG is mainly concentrated in Unit 1 (28–100 cm).

Correlation analyses between the grain-size end members and the traditional grain-size parameters showed that EM1 and EM2 were composed of clay and fine silt with fine grain sizes of 0.04 μm and 9.8 μm, respectively. These end members were deposited under the weak hydrodynamic conditions of long-distance transport along the Yellow River. EM3 and EM4 were coarse silt with mode grain sizes of 40.14 μm and 66.89 μm, respectively. They were deposited by waves and tidal currents under strong hydrodynamic conditions.

The grain-size parameters of cores YDC and YDG can accurately record the information of the Yellow River diversion and the change of sedimentary environment, and the 28 cm can be used as a reference point. Cores YDC and YDG belong to the delta-plain and delta-front facies, respectively. Before the Yellow River was diverted to the Qing 8 course in 1996, cores YDC and YDG were in the delta-front estuary bar sedimentary environment. The contents of clay and fine silt and the EM1 and EM2 components were higher in the sediments, which reflects the abundant input of Yellow River sediment. In 1996, when the Yellow River was diverted, the content of clay decreased, and the contents of silty sand and sand increased in core YDC. The contents of EM3 and EM4 representing coarse-grained components rapidly increased, while the contents of EM1 and EM2 representing fine-grained components rapidly decreased. However, the content of clay in core YDG rapidly increased and the contents of silty sand and sand decreased. EM1 and EM2, which represent the fine-grained components, increased rapidly, and were dominated by tidal currents and suspended sediment diffusion and deposition. The sediment source changed in 1996 from the Yellow River sediment to coastal sediment and the sedimentary environment changed from siltation to erosion.

## Data availability statement

The original contributions presented in the study are included in the article/supplementary material. Further inquiries can be directed to the corresponding author.

## Author contributions

LM and LW designed the research and wrote the manuscript. JZ software analysis and application. LW, CZ, XL and BC collected cores YDC and YDG analyzed the sedimentary sequences of the driling cores. LZ and QW refined the interpretations. All authors reviewed the manuscript. All authors contributed to the article and approved the submitted version.

## Funding

This research was supported financially by National Natural Science Foundation of China (No. 41702185, U1706220), the Foundation of School and Land Integration Development in Yantai (NO. 2021XDRHXMQT18), the open foundation of State Key Laboratory of Lake Science and Environment (No. 2022SKL005), the open foundation of CAS Key Laboratory of Coastal Environmental Processes and Ecological Remediation, YICCAS (NO. 2020KFJJ10), the open foundation of State Key Laboratory of Loess and Quaternary Geology, Institute of Earth Environment, CAS (NO. SKLLQG2024). Youth Innovation Team Project for Talent Introduction and Cultivation in Universities of Shandong Province, Key project of Research and Development Program in Shandong Province (NO. 2022RKY07006).

## Conflict of interest

The authors declare that the research was conducted in the absence of any commercial or financial relationships that could be construed as a potential conflict of interest.

## Publisher's note



## References

Chen, H., Kong, F., Xu, S., and Miao, X. (2021). Dust accumulation process indicated by grain size end-members of the coastal loess since the late pleistocene in miaodao islands of Shandong province. *Quaternary Sci.* 41 (05), 1306–1316. doi: 10.11928/j.issn.1001-7410.2021. 05.07

Chen, T., Liu, Q., and Zheng, Y. (2021). Environmental magnetic properties of core sediments in the yellow river subaqueous delta and their chronological applications. *Chin. Sci. Bull.* 66 (30), 3902–3915. doi: 10.1360/TB-2021-0528

Chen, J., Yang, T., Qiang, M., Matishov, G. G., and Shi, P. (2020). Interpretation of sedimentary subpopulations extracted from grain size distributions in loess deposits at the Sea of Azov, Russia. *Aeolian Res.* 45, 100597. doi: 10.1016/j.aeolia.2020.100597

Dethier, E. N., Renshaw, C. E., and Magilligan, F. J. (2022). Rapid changes to global river suspended sediment flux by humans. *Science* 376 (6600), 1447–1452. doi: 10.1126/science.abn7980

Han, G., Li, Y., Yu, J., Xu, J., Wang, G., Zhang, Z., et al. (2011). Evolution process and related driving mechanisms of yellow river delta since the diversion of yellow river. *Chin. J. Appl. Ecol.* 22 (02), 467–472. doi: 10.13287/j.1001-9332.2011.0047

Hou, C., Yi, Y., Song, J., and Zhou, Y. (2021). Effect of water-sediment regulation operation on sediment grain size and nutrient content in the lower yellow river. *J. Cleaner Production* 279, 123533. doi: 10.1016/j.jclepro.2020.123533

Hu, N. J., Huang, P., Liu, J. H., Shi, X. F., Ma, D. Y., Zhu, A. M., et al. (2015). Tracking lead origin in the yellow river estuary and nearby bohai Sea based on its isotopic composition. *Estuar. Coast. Shelf Sci.* 163 (SEP.20PT.B), 99–107. doi: 10.1016/j.ecss.2015.06.010

Hu, G., Zhang, Y., Kong, X., Wu, X., Wang, Z., Yuan, Z., et al. (2021). Changes of evolution models of china's large river deltas since Holocene and their responses to anthropogenicactivities. *Mar. Geology Quaternary Geology* 41 (05), 77–89. doi: 10.16562/j.cnki.0256-1492.2020122201

Hu, C., Zhang, X., and Zhao, Y. (2020). Cause analysis of the centennial trend and recent fluctuation of the yellow river sediment load. *Adv. Water Sci.* 31 (05), 725–733. doi: 10.14042/j.cnki.32.1309.2020.05.009

Jiang, C., Chen, S., Pan, S., Fan, Y., and Ji, H. (2018). Geomorphic evolution of the yellow river delta: Quantification of basin-scale natural and anthropogenic impacts. *Catena* 163, 361–377. doi: 10.1016/j.catena.2017.12.041

Jia, Y. G., Wu, Q., Shang, H., Yang, Z. N., and Shan, H. X. (2011). The influence of oil contamination on the geotechnical properties of coastal sediments in the yellow river delta, China. *Bull. Eng. Geology Environ.* 70 (3), 517–525. doi: 10.1007/s10064-011-0349-8

Li, S. (1989). Sedimentary characteristics in the modern yellow river delta. *Geographical Res.* 04), 45–55.

Li, G., Chen, S., Peng, J., Chen, X., Liu, F., and Chen, G. (2013). Sedimentary environment analysis of drilling core YDZ1 from the yellow river delta. *Adv. Mar. Sci.* 31 (02), 205–212.

Li, Y., Song, Y., Zong, X., Zhang, Z., and Cheng, L. (2019). Dust accumulation processes of piedmont loess indicated by grain-size end members in northern lli basin. *Acta Geographica Sin.* 74 (01), 162–177. doi: 10.11821/dlxb201901012

Liu, M., Li, X., Han, Z., Chen, Y., Wang, Y., Yuan, X., et al. (2021). Parametric end-member analysis of the grain size distribution of the xiashu loess and its provenance tracing. *J. Earth Environ.* 12 (05), 510–525. doi: 10.7515/JEE212015

Liu, T., Shi, X., Li, C., and Yang, G. (2012). The reverse sediment transport trend between abandoned huanghe river (Yellow river) delta and radial sand ridges along jiangsu coastline of China–an evidence from grain size analysis. *Acta Oceanol. Sin.* 31 (6), 83–91. doi: 10.1007/s13131-012-0255-3

Liu, R., Yue, D., Zhao, J., Su, Z., Shi, H., and Wang, X. (2021). Characterisitics of grain size end members and its environmental significance of aeolian sand/loess sedimentary sequence since L2 in hengshan, shaanxi province. *Arid Land Geogr.* 44 (05), 1328–1338. doi: 10.12118/j.issn.1000-6060.2021. 05.14

Liu, L., Wang, H., Yang, Z., Fan, Y., Wu, X., Hu, L., et al. (2022). Coarsening of sediments from the Huanghe (Yellow River) delta-coast and its environmental implications. *Geomorphology* 401, 108105. doi: 10.1016/j.geomorph.2021.108105

Li, S., Wang, H., Zhang, Y., Bi, N., Wu, X., and Hu, B. (2015). Variation in sediment load and grain-size under the influence of water and sediment regulation scheme (wsrs)of the huanghe (Yellow). *Mar. Geology Front.* 31 (07), 20–27. doi: 10.16028/j.1009-2722.2015.07003

Li, G., Wei, H., Yue, S., Cheng, Y., and Han, Y. (1998). Sedimentation in the yellow river delta, part II: suspended sediment dispersal and deposition on the subaqueous delta. *Mar. Geology* 149 (1), 113–131. doi: 10.1016/S0025-3227(98)00032-2

McCave, I. N., and Swift, S. A. (1976). A physical model for the rate of deposition of fine-grained sediments in the deep sea. *Geological Soc. America Bull.* 87 (4), 541–546. doi: 10.1130/0016-7606(1976)87<541:APMFTR>2.0.CO;2

Milliman, J. D., and Meade, R. H. (1983). World-wide delivery of river sediment to the oceans. *J. Geology* 91 (1), 1–21. doi: 10.1086/628741

Paladino, Í.M., Mengatto, M. F., Mahiques, M. M., Noernberg, M. A., and Nagai, R. H. (2022). End-member modeling and sediment trend analysis as tools for sedimentary processes inference in a subtropical estuary. *Estuarine Coast. Shelf Sci.* 278, 108126. doi: 10.1016/j.ecss.2022.108126

Pan, B., Pang, H., Zhang, D., Guan, Q., Wang, L., Li, F., et al. (2015). Sediment grain-size characteristics and its source implication in the ningxia–inner Mongolia sections on the upper reaches of the yellow river. *Geomorphology* 246, 255–262. doi: 10.1016/j.geomorph.2015.06.028

Paterson, G. A., and Heslop, D. (2015). New methods for unmixing sediment grain size data. *Geochemistry* 16 (12), 4494–4506. doi: 10.1002/2015GC006070

Qiao, S., Shi, X., Zhu, A., Liu, Y., Bi, N., Fang, X., et al. (2010). Distribution and transport of suspended sediments off the yellow river (Huanghe) mouth and the nearby bohai Sea. *Estuarine Coast. Shelf Sci.* 86 (3), 337–344. doi: 10.1016/j.ecss.2009.07.019

Shi, C. (2021). Deposition and dispersal of different grain-size sediments in the yellow river estuary. *Geographical Res.* 40 (04), 1125–1133. doi: 10.11821/dlyj020200203

Van Hateren, J. A., Prins, M. A., and van Balen, R. T. (2018). On the genetically meaningful decomposition of grain-size distributions: A comparison of different end-member modelling algorithms. *Sedimentary Geology* 375, 49–71. doi: 10.1016/j.sedgeo.2017.12.003

Varga, G., Jvári, G., and Kovács, J. (2019). Interpretation of sedimentary (sub) populations extracted from grain size distributions of central European loess-paleosol series. *Quaternary Int.* 502, 60–70. doi: 10.1016/j.quaint.2017.09.021

Wang, H., Bi, N., Saito, Y., Yan, W., Sun, X., Zhang, J., et al. (2010). Recent changes in sediment delivery by the huanghe (Yellow river) to the sea: Causes and environmental implications in its estuary. *J. Hydrology* 391 (3-4), 302–313. doi: 10.1016/j.jhydrol.2010.07.030

Wang, Z., Huang, C., Yang, H., Pang, J., Cha, X., and Zhou, Y. (2018). Loess provenance characterlstlcs and evolution indlcated by graln SizeSince late pleistocene at the Eastern foot of liupan mountains, China. *Scientia Geographica Sin.* 38 (05), 818–826. doi: 10.13249/j.cnki.sgs.2018.05.020

Wang, H., Xiao, W., Bi, N., Song, L., and Nittrouer, J. (2017). Impacts of the dam-orientated water-sediment regulation scheme on the lower reaches and delta of the yellow river (Huanghe): A review. *Global Planetary Change* 157, 93–113. doi: 10.1016/j.gloplacha.2017.08.005

Wang, Z., Yu, D., Wang, W., Luo, F., Tang, J., and Yang, J. (2021). End-member analysis of sedimentary dynamics indicated by the grain-size of surface sediments in the quanzhou bay. *Trop. Geogr.* 41 (05), 975–986. doi: 10.13284/j.cnki.rddl.003377

Wang, W., Zhou, L., Duan, Z., Jiang, Z., Liu, J., and Liu, Q. (2019). Magnetostratigraphic framework and magnetic properties of modern sediment in the yellow river delta. *Chin. J. Geophys.* 62 (05), 1772–1788. doi: 10.6038/cjg2019M0158

Wen, Y., Wu, Y., Tan, L., Li, D., and Fu, T. (2019). End-member modeling of the grain size record of loess in the mu us desert and implications for dust sources. *Quaternary Int.* 532, 87–97. doi: 10.1016/j.quaint.2019.10.005

Wu, X., Bi, N., Xu, J., Nittrouer, J. A., Yang, Z., Saito, Y., et al. (2017). Stepwise morphological evolution of the active yellow river (Huanghe) delta lobe, (1976–2013): Dominant roles of riverine discharge and sediment grain size. *Geomorphology* 292, 115–127. doi: 10.1016/j.geomorph.2017.04.042

Wu, X., Fan, Y., Wang, H., Bi, N., Xu, C., Zhang, Y., et al. (2021). Evolution of abandoned deltaic river channel–a case from the diaokou channel of the yellow river. *Mar. Geology Quaternary Geology* 41 (02), 22–29. doi: 10.16562/j.cnki.0256-1492.2020070101

Wu, X., Wang, H., Bi, N., Nittrouer, J. A., and Li, Z. (2020). Evolution of a tide-dominated abandoned channel: A case of the abandoned qingshuigou course, yellow river. *Mar. Geology* 422 (7–26), 106116. doi: 10.1016/j.margeo.2020.106116

Xu, J. (2000). Grain-size characteristics of suspended sediment in the yellow river, China. *Catena* 38 (3), 243–263. doi: 10.1016/S0341-8162(99)00070-3

Xue, C., Ye, S., Gao, M., and Ding, X. (2009). Determination of depositional age in the huanghe delta in China. *Acta Oceanol. Sin.* 31 (01), 117–124.

Yuan, P., Bi, N., Wu, X., Zhang, Y., and Wang, H. (2016). Surface sediments at the subaqueous yellow river delta:classification and distribution. *Mar. Geology Quaternary Geology* 36 (02), 49–57. doi: 10.16562/j.cnki.0256-1492.2016.02.006

Zang, X., Ji, Y., Yang, Z., Wang, Z., Liu, D., and Jia, P. (2015). End element inversion of grain size in surface sediments of the south yellow Sea and its implications for sedimentary dynamic environment. *Scientia Sinica(Terrae)* 45 (10), 1515–1523. doi: 10.1007/s11430-015-5165-8

Zeng, L., Wang, Q., Zhan, C., Liu, X., Wang, L., Cheng, S., et al. (2022). Geomorphologic evolution of the abandoned yellow river delta during the last 2000 years. *Front. Mar. Sci.*, 2512. doi: 10.3389/fmars.2021.761368

Zhang, X., Wang, H., Xu, S., and Yang, Z. (2020). A basic end-member model algorithm for grain-size data of marine sediments. *Estuarine Coast. Shelf Sci.* 236, 106656. doi: 10.1016/j.ecss.2020.106656

Zhang, J., Xiao, H., and Zhang, X. (2020). An analysis of the impact of the longyangxia reservoir on the variation of runoff and sediment load conditions downstream. *China Rural Water Hydropower* 01), 83–87.

Zhang, Y., Yu, J., Ren, Z., Wang, H., Xu, G., Zhan, C., et al. (2022). Influence of reduced sediment supply on the particle size distribution on tidal flats of the yellow river delta: A physical experimental study. *Mar. Geology Front.* 38 (06), 34–46. doi: 10.16028/j.1009-2722.2022.007

Zhang, X., Zhai, S., and Xu, S. (2006). The application of grain-size end-member modeling to the shelf near the estuary of changjiang river in China. *Acta Oceanol. Sin.* 04), 159–166.

Zhong, N., Jiang, H., Li, H., Xu, H., Liang, L., and Shi, W. (2020). End member inversion of xinmocun lacustrine sediments in the upper reaches of the minjiang river and its recorded tectonic and climate events. *Acta Geologica Sin.* 94 (03), 968–981. doi: 10.19762/j.cnki.dizhixuebao.201909